system containing N-methylphenothiazine and methyl viologen. The transient absorption at 530 nm probably is a composite of the absorption due to PTD cation radical and Ru(bipy)$_2$ (dhbipy),$^+$ and that at 450 nm probably is due to PTD triplet state.[5] No such absorption was observed without PTD or Ru(bipy)$_2$ (dhbipy)$^{2+}$ in the vesicle. Thus the excited state of ruthenium complex with two long hydrocarbon chains was quenched reductively by PTD in the vesicle system. The PTD cation radical is involved in the hydrogen generation vesicle system. The data of absorption decay kinetics were too poor to give consistent fits, but using different portions of the data, estimates for life time could be obtained. That indicates a value in the 4-8 msec range. (see Figure 4 and Figure 5) Also, we saw what appeared to be very weak slow component in the logarithmic plot of the decay. An estimate of the life time of this decay might be of order 20-40 msec. Probably the life of the PTD cation radical is longer in aquous portion than hydrophobic portion. The oxidized PTD cation radical escapes into aquous portion of the

References

1. M. Calvin, *Accts. Chem. Res.*, **11**, 369-374 (1978).
2. M. S. Tunuli, and *J.* H. Fendler J. *Amer. Chem. Soc.*, **103**, 2507 (1981).
3. J. H. Fendler, *J. Phys. Chem.*, **89**, 2730 (1985).
4. Y.-T. Park, *Bull. Korean Chem. Soc.*, **4**, 149 (1983).
5. P. P. Infelta, M. Gratzel, and J. H. Fendler, *J. Amer. Chem. Soc.*, **102**, 1479 (1980).
6. F. E. Lytle and D. M. Hercules, *J. Amer. Chem. Soc.*, **91**, 253 (1969).
7. Kiwi J. and M. Gratzel *J. Amer. Chem. Soc.*, **100**, 6314 (1978).

Substitution Reaction of Fe(CO)₅ by Ethylene

Jaejung Ko

Department of Chemical Education, Korea National University of Education,
Choongbuk 363-890. Received November 9, 1987

The substitution reaction of Fe(CO)₅ by ethylene has been studied for plausible intermediates by means of extended Huckel calculations. Among various reaction mechanisms the favorable reaction pathway is via a dissociative mechanism in which ethylene approaches to Fe(CO)₄ unit. For Fe(CO)₄ fragment, the square planar conformation is found to be the most stable form by the extended Huckel calculations. Our calculations show that ethylene attacks square planar intermediate formed by removing one carbonyl from Fe(CO)₅ and then the unstable species thus formed is distored to the most stable trigonal bipyramid with the ethylene lying in the equatorial plane.

Introduction

Process in which complexes undergo ligand substitution reaction is the most important step in organometallic mechanisms. A delineation of the mechanisms by which these processes occur is vital to a full understanding of the chemistry of complexes.[1] The majority of proposed mechanisms require at least one ligand substitution steps via D, I_d, I_a, or A mechanism.[2] It is well documented[3] that 18 electron ML_6 and 16 electron ML_4 complexes in the organometallic ligand substitution reactions proceed with a dissociative (D or I_d) and an associative mechanism (A or Ia), respectively, albeit considerable ambiguity. Recent reports[4] on the ligand substitution reaction indicate that while 18 electron ML_5, and ML_4 complexes proceed with a dissociative mechanism via a 16 electron intermediate, there still be considerable conflict. Therefore, we chose the system which treats the reaction of Fe(CO)₅ with C_2H_4 because first, we are interested in mechanistic studies on 18 electron ML_5 complexes in order to check whether the system proceeds with a dissociative or associative mechanism, and secondly, little theoretical work has been brought to bear on this subject, and finally, complexes of type Fe(CO)₄ (η^2-hydrocarbon) are easily accessible.[5]

The principal substitution process is the replacement of CO by C_2H_2 to form the stable monoethylene complex:

$$Fe(CO)_5 + C_2H_4 \rightarrow Fe(CO)_4(C_2H_4) + CO$$

As likely mechanisms for this overall reactions, five mechanisms can be proposed as shown below (1a-e). The first three mechanism is the transient intermediate of reduced coordination number, giving rise to a D mechanism. The last two (1d-e) mechanism is a fully formed intermediate complex, so-called A mechanism. Therefore, computational calculations on each intermediate will help clarify the energetics of this reaction type as well as provide data for transition
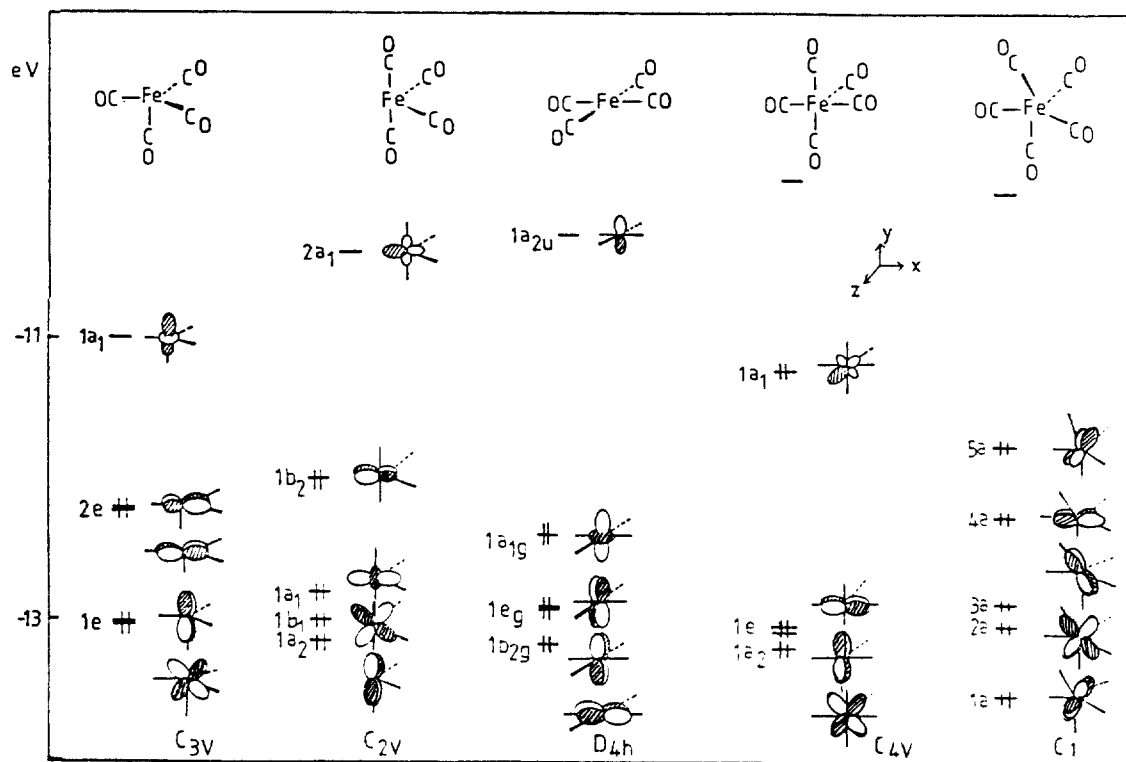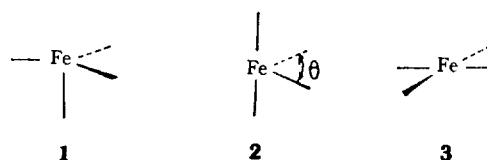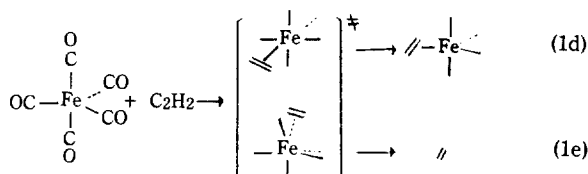
88 *Bull. Korean Chem. Soc., Vol. 9, No. 2, 1988*

Jaejung Ko
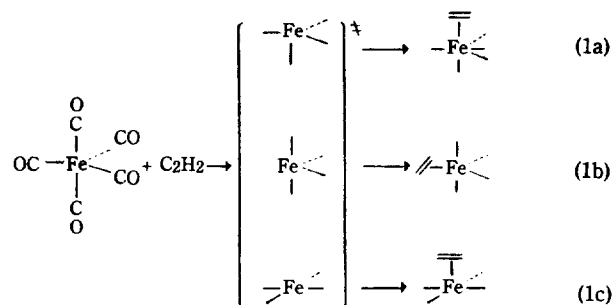
Figure 1. Important Valence orbitals of five Fe(CO)4-5 fragments.

state geometrics, leading to understand the reaction mechanism.

In this paper, we describe a mechanistic study on the substitution reaction of $Fe(CO)_5$ with C_2H_4 by means of extended Hückel calculations.

Fe(CO)4.5 Fragments

For mechanistic studies on the reaction of $Fe(CO)_5$ with C_2H_4, five mechanisms can be proprosed as discussed in the introduction section. In order to compare the stability and electronic structure of each intermediate, a computational calculation was carried out on each instance. Our actural calculations are of the extended Hückel type, with parameters specified in the Appendix.

A natural framework for the mechanism of $Fe(CO)_4(C_2H_4)$ complex is found in the conceptional construction of the complex from $Fe(CO)_5$ and ethylene fragments. The MOs of the $Fe(CO)_{4-5}$ fragments are developed and interacted with the levels of the ethylene. The valence orbitals of five $Fe(CO)_{4-5}$ fragments are shown in Figure 1.

The tetracoordinate fragment geometries, 1 and 2 were derived by removing one axial or equatorial carbonyl ligand from a trigonal bipyramid ML_5, respectively. The square-planar structure can be obtained by opening up one angle of 2, θ, from 120° to 180°. In the C_{3v} $Fe(CO)_3$ fragment there are two sets(e) of low-lying occupied levels. The high-lying e

orbitals are formed from a conbination of metal-based xy and x^2-y^2 orbitals as the HOMO and have δ symmetry with respect to an incoming ethylene. There is a high-lying $1a_1$ orbital composed mainly of z^2, s and z on the metal as the LUMO. In the C_{2v} $Fe(CO)_4$ fragment there are four low-lying, occupied orbitals. The HOMO can be thought as representing a π bond $1b_2$ orbital formed from the combination of xy and y orbitals. The difference in energy between $1a_1$ and $1a_2$ orbitals is relatively small. The $1a_1$ and $1a_2$ orbitals have σ and δ symmetry for an incoming ligand. The $1b_1$ and $1b_2$ orbitals have a large energy difference and hybridization difference. If an ethylene with π orbital which is antisymmetric with respect to the xz plane approaches to the $Fe(CO)_4$ fragment, it will interact with $1b_2$. Upon rotation by 90° the π orbital will interact with $1b_1$. These orbitals are marked resemblance with those of the $Ni(CO)_2$ fragments[6]. The D_{4h} $Fe(CO)_4$ fragment is most clearly related to the D_{4h} square-planar $M(CO)_4$[7]. There are four levels, $b_{2g} + e_g + 2a_{1g}$, which are primarily metal in character and lie at moderate energy.

Now we turn to the total energy of each $Fe(CO)_4$ intermediate. The total energy of C_{3v}, C_{2v}, and D_{4h} $Fe(CO)_4$ fragments is -906.37, -907.09, and -907.53 eV, respectively. On energy grounds, the most stable intermediate is the D_{4h} $Fe(CO)_4$ fragment. The difference in energy between the HOMO and LUMO for C_{3v}, C_{2v}, and D_{4h} $Fe(CO)_4$ fragments is 1.2 eV, 1.6 eV, and 2.1 eV, respectively. Therefore, among the intermediates formed by removing one carbonyl ligand

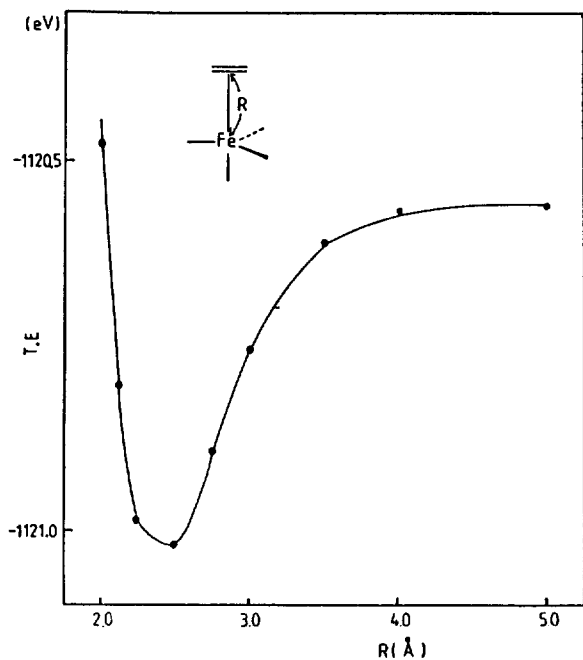**Figure 2.** Potential curve for the distance between ethylene and iron [C_{3v} Fe(CO)₄].

from a trigonal pyramid, the square planar D_{4h} Fe(CO)₄ fragment is the most stable form energetically and electronically. We would say that if the reaction proceeds with a dissociative mechanism, first, one carbonyl ligand is removed and then the structure is distorted to the most stable square-planar Fe(CO)₄ fragment via a C_{4r} square-pyramidal structure, as shown below.
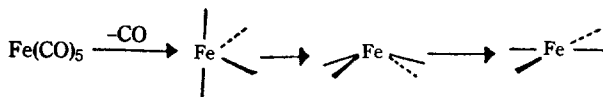
The pentacoordinate fragment geometries were derived from the trigonal bipyramid by making a slight geometrical distortion. The C_{4v} Fe(CO)₅ fragment can be obtained by
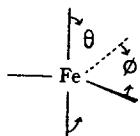
squeezing one angle, ϕ, from 120° to 90° and the C_1 Fe(CO)₅ fragment by bending one angle, θ, from 180° to 120°. The C_{4v} Fe(CO)₅ fragment is closely related to an octahedral complex.[8] There is a lower set of three levels e + a₂, descended from the octahedral t_{2g}. The xz and yz components of t_{2g} would rise slightly in energy and xy is left untouched. A relatively small energy gap will be introduced between e and b₂. At much higher energy is x^2-y^2, which along with 1a₁ formed the e_g in ML₆. The a₁ orbital becomes hybridized by mixing some s, z, and z^2 character.

The difference in energy between the HOMO and LUMO for C_{4v} and C_1 Fe(CO)₅ fragments is 1.33 and 1.76 eV, respectively. The total energy of C_{4v} and C_1 Fe(CO)₅ fragments is -1106.95 and -1104.74 eV, respectively. Although C_1 Fe(CO)₅ fragment is more stable than C_{4v} Fe(CO)₅ fragment electronically, the reason that C_{4v} Fe(CO)₅ fragment is more
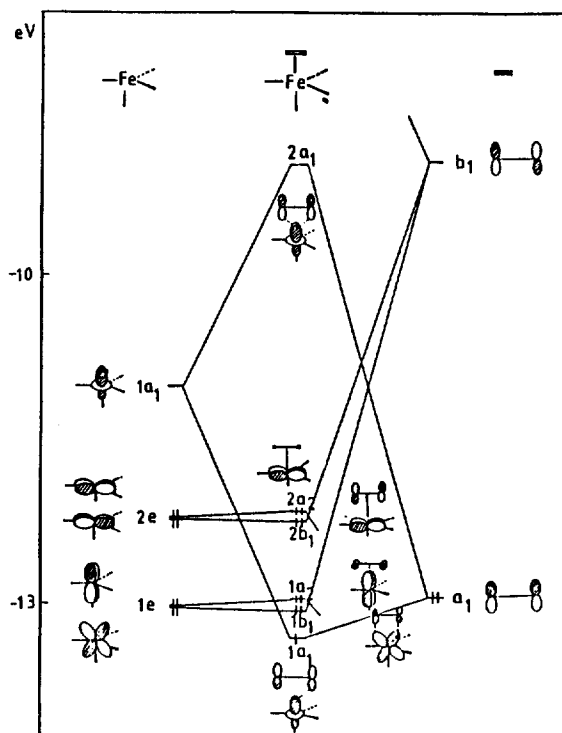
Figure 3. Correlation diagram of orbitals of Fe(CO)₄(C₂H₄) with those of the singlet fragments.

stable energetically can be explained by a higher set of two levels 3a + 2a, desended from the C_{4v} Fe(CO)₄ fragment 1e. With these orbitals in mind, we not turn our attention to the ethylene complexes.

Fe(CO)₄(C₂H₄) complex

(1) Interaction of C_{3v} Fe(CO)₄ unit with ethylene (1a). Figure 2 shows the potential curve as a function of R when ethylene approaches to the axial position of C_{3v} Fe(CO)₄ fragment. The geometrical optimization afforded the value R = 2.45 Å. Figure 3 shows the interaction diagram for an ethylene ligand and a C_{3v} Fe(CO)₄ fragment at the transition state. At the right of the Figure are symmetry adapted linear combination of the P_π hybrids on each carbon atom. The 1a₁ orbital on ethylene interacts with metal centered 1a₁ orbital in a bonding and antibonding fashion to produce a Fe-C σ and σ^* bonds, labelled the 1a₁ and 2a₁ on the center, respectively. At higher energy the 1b₁ orbital on ethylene interacts with xz and xy in a bonding fashion. The 2a₂ orbital is essentially nonbonding as the HOMO. The HOMO-LUMO gap is large (3.16 eV), which makes the complex stable at least electronically.

(2) Interaction of C_{2v} Fe(CO)₄ fragment with ethylene (1b). Figure 4 shows the potential curve with the bond length R. The optimum bond length was calculated to have R = 2.25 Å. The bond length can be reduced to 2.05 Å with use of the optimized parameters, which is very close to that obtained by gas-phase electron diffraction studies.[15] Figure 5 shows the interaction diagram for an ethylene ligand and a C_{2v} Fe(CO)₄ unit. Although this qualitative analysis was already reported[6], we will review the molecular interaction for comparison with other cases. A large number of X-ray st-
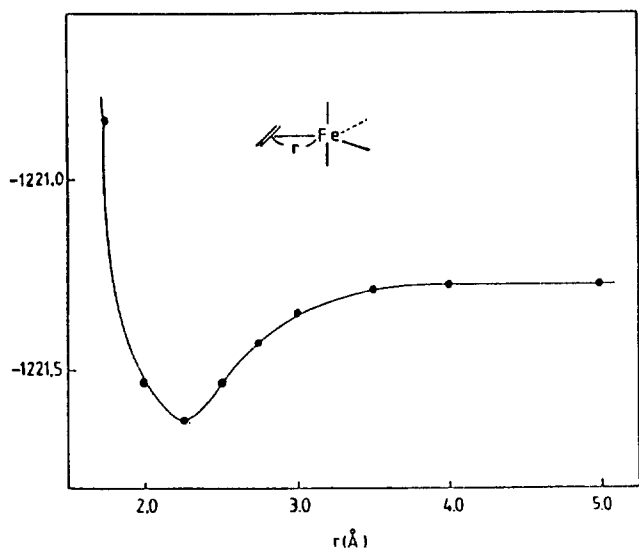
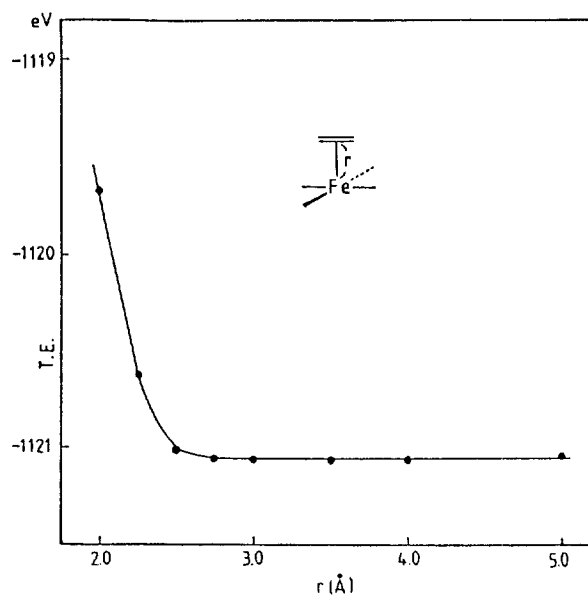90 *Bull. Korean Chem. Soc., Vol. 9, No. 2, 1988*

Jaejung Ko

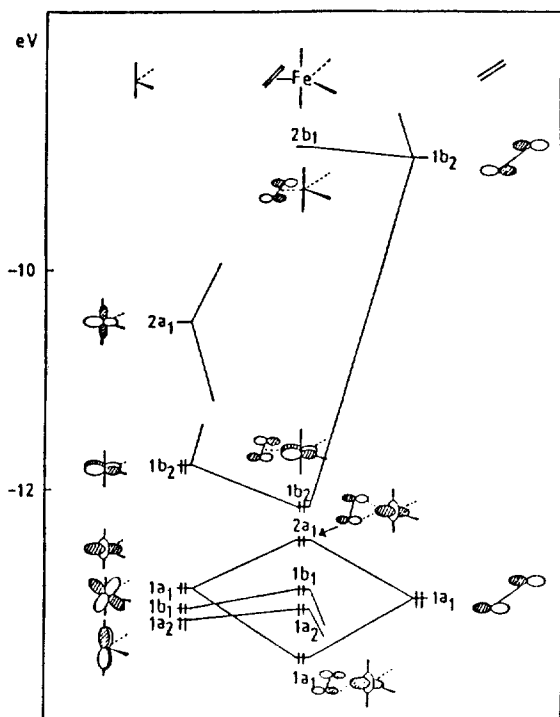**Figure 4.** Potential curve for the distance between ethylene and iron [C_{2v} Fe(CO)$_4$].

Figure 5. Interaction diagram for Fe(CO)$_4$(C$_2$H$_4$).

ructure[9] has shown that the most stable conformation of ethylene-Fe(CO)$_4$ is the trigonal bipyramid which the ethylene ligand lies in the trigonal in-plane conformation as in 4. Upon rotation of ethylene by 90°, the in-plane conformation was transformed into the upright one as in 5. From our calculations, the in-plane structure, 4, was calculated to be 29.21 kcal/mol more stable than the upright one 5. The value was in a quantitative agreement with that of *ab initio* level[10]

4   **5**

Figure 6. Potential curve for the distance between ethylene and iron [D_{4h} Fe(CO)$_4$].

To understand a ratational process, let's return to the interaction diagram for two extreme geometries. As shown in Figure 4, the ethylene π donor orbital, 1b$_1$, interacts with the 1b$_2$ of a C_{2v} Fe(CO)$_4$ fragment to produce π bonding, 2b$_1$, as the HOMO. The 1b$_2$ orbital of Fe(CO)$_4$ unit is made up of metal xy and y as in 6. Therefore, the interaction of 1b$_1$ with

6
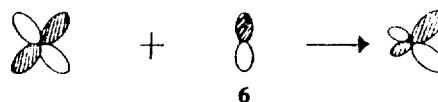
an ethylene orbital will give an effective overlap as in 7. In contrast to that, the 1a$_1$ of a C_{2v} Fe(CO)$_4$ fragment interacts with the ethylene π donor, 1b$_1$, to produce the 1b$_1$ orbital(8) of Fe(CO)$_4$ (C$_2$H$_4$) complex. Accordingly, we would say that the 1b$_2$ orbital strongly interacts with the corresponding orbital of ethylene compared with that of the 1b$_1$ orbital. That mainly leads to a conformational preference.

7   **8**

(3) Interaction of D$_{4h}$ Fe(CO)$_4$ fragment with ethylene (1C). For intermediates formed by removing one carbonyl ligand from Fe(CO)$_5$ complex, we have calculated the lowest energy structure of Fe(CO)$_4$ by the extended Hückel calculation. We find the most favorable geometry to be square planar. This result agrees with that calculated in the intermediate arising from the subsititution of CO for C$_2$H$_4$ in Fe(CO)$_3$(C$_2$H$_4$)$_2$[11]. Now consider the approach of ethylene to D$_{4h}$ Fe(CO)$_4$. Figure 6 shows the potential curve as a function
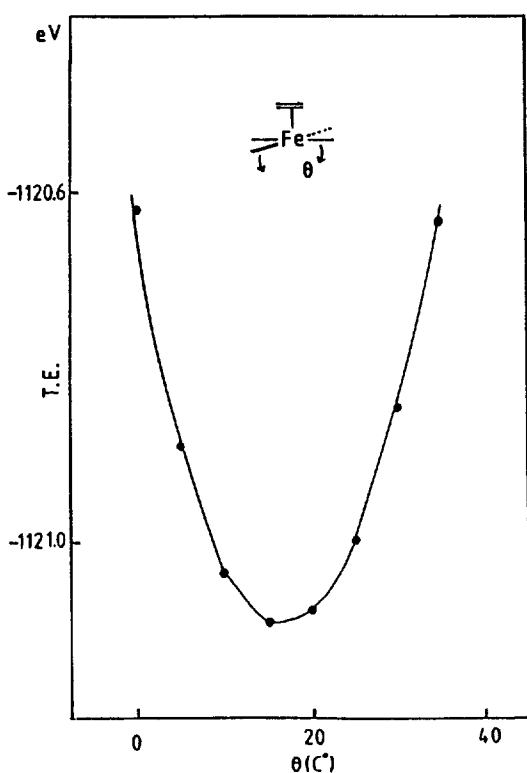

9   **10**
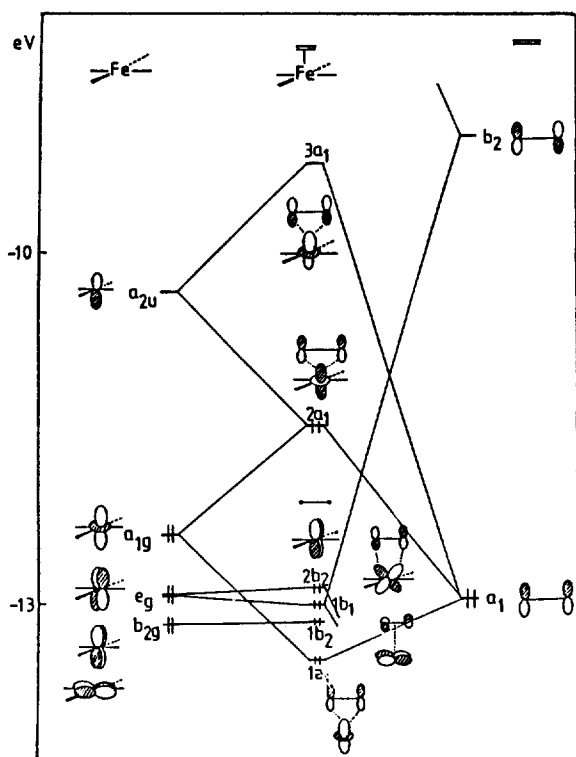
Figure 7. Potential curve for the change of angle.

Figure 8. Correlation diagram of orbitals of $Fe(CO)_4(C_2H_4)$ with D_{4h} $Fe(CO)_4$ and C_2H_4.

of R as in 9. Figure 7 shows the potential curve as an angle of θ with the optimized distance fixed as in 10. The optimum angle was calculated to be $\theta = 16°$. Figure 8 shows the interaction diagram for an ethylene and a D_{4h} $Fe(CO)_4$ unit. At

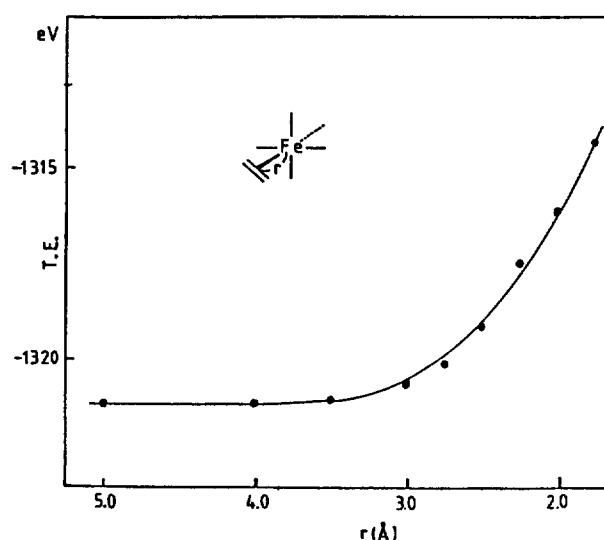**Figure 9.** Potential curve for the distance between ethylene and iron [C_{4v} $Fe(CO)_5$].

lower energy a_1 mixes with z^2 in a bonding fashion to produce a Fe-C σ bond, $1a_1$. At higher energy a_1 interacts with z^2 in an antibonding fashion to produce a Fe-C σ^* bond, $2a_1$, as the HOMO. A striking aspect of this analysis is that the a_1 orbital interacts with z^2 to produce filled bonding and antibonding molecular interaction is more destabilized than the bonding interaction is stabilized, in the case, the net interaction between a_1 and z^2 is attractive. This may be attributable to the reduction of antibonding character by the resultant orbital of the a_{2u} and a_{1g} orbitals as in 11. As ethylene ap-

11
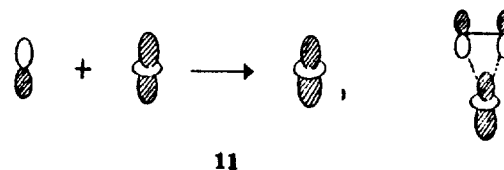
proaches to a $Fe(CO)_4$ unit, the $2a_1$ orbital will rise to a high energy due to the strong interaction between a_1, a_{1g}, and a_{2u} orbitals. Therefore, an obvious way to elude the antibonding interaction would allow the Fe-C distance to increase or the geometrical perturbation to occur. If the geometrical perturbation occurs from 9 to 4, the antibonding orbital, $2a_1$, of 9 is transformed to the bonding orbital, $1b_2$, of 4. This may be the driving force which the unstable intermediate, 9, is distorted to the most stable conformation, 4.

We now turn to the geometrical stability of the $Fe(CO)_4$-ethylene complex (1a-c). We will examine the barrier in a stepwise manner. From our calculations, the most stable conformation is shown to be C_{2v} $Fe(CO)_4(C_2H_4)$ complex. The total energy of 4 is -1121.63 eV. It requires 12.58 and 10.95 kcal/mol to distort 4 to a square pyramidal geometry, 10, and C_{3v} $Fe(CO)_4(C_2H_4)$ complexes, respectively. On distorting 10 to 9, it requires 14.6 kcal/mol. Therefore, we would say that if the reaction proceeds with a dissociative mechanism, ethylene attacks the most stable intermediate D_{4h} $Fe(CO)_4$ and then a relatively unstable conformation, 9, is easily transformed into the trigonal bipyramid with the ethylene lying in the equatorial plane with energy gain.
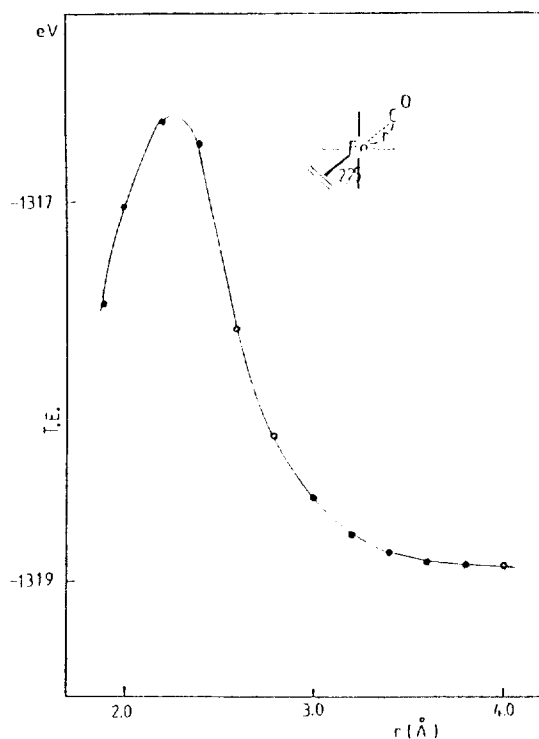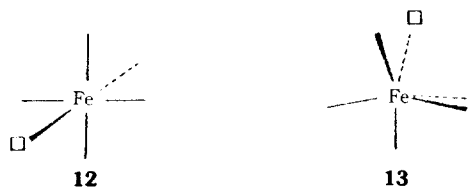
92 *Bull. Korean Chem. Soc., Vol. 9, No. 2, 1988*

Jaejung Ko

Figure 10. Potential curve for the distance between carbon and iron.

Figure 11. Potential curve for the distance between ethylene and iron [C₁ Fe(CO)₅].

Fe(CO)₅(C₂H₄) intermediate

An alternative mechanism on substitution reaction of Fe(CO)₅ with ethylene is of an associative mechanism in which Fe(CO)₅ is perturbed to 12 or 13 for an incoming ligand. Figure 9 shows the potential curve when ethylene ap-

proaches to a vacant site (shown by □) of 12. As shown in Figure 9, it appears that in the transition state for the ethylene addition to 12 the Fe(CO)₅(C₂H₄) intermediate becomes unstable as the distance between iron and ethylene comes close. For a reasonable approach of ethylene to iron metal to occur, the bond between carbonyl trans to ethylene and iron has to become activated, giving rise to a bond lengthening via an I₍ₐ₎ mechanism (14) and then the carbonyl ligand easily disappears without any energy addition. The resulting intermediate Fe(CO)₄(C₂H₄) will rearrange to the most stable trigonal pyramid conformation with energy gain. We now turn to the process of removing one carbonyl ligand from Fe(CO)₅(C₂H₄). Figure 10 shows the potential curve when the carbonyl group trans to ethylene disappears with the distance between ethylene and iron fixed (2.25 Å). From Figure 10 we calculate that the activation energy is 22.6 kcal/mol. In the activated state the distance between carbon and iron is over 2.25 Å, the carbonyl ligand is spontaneously disappears. In the case of the intermediate in which ethylene approaches to C₁ Fe(CO)₅ fragment, the pattern is very similar to the C₄ᵥ Fe(CO)₅ intermediate. Figure 11 shows the potential curve as

a function of distance which ethylene approaches to a vacant site of 13 (shown by □). The activation energy as an apical carbonyl group near ethylene is removed is calculated to be 21.3 kcal/mol. Therefore, we would say that when the reaction proceeds with an associative mechanism with 20 electron configuration, the process of removing one carbonyl group meets with an activation state. We now reexamine two processes proceeding with an associative mechanism from geometrical perturbation to rearrangement process. When the trigonal bipyramid Fe(CO)₅ complex is distorted to 12 and 13, it requires 24.93 and 76.42 kcal/mol, respectively. The next step is that ethylene approaches to the perturbed conformations, 12 and 13 to become activated states, 14 and 15. In the activated states, 14 and 15, two obvious ways to
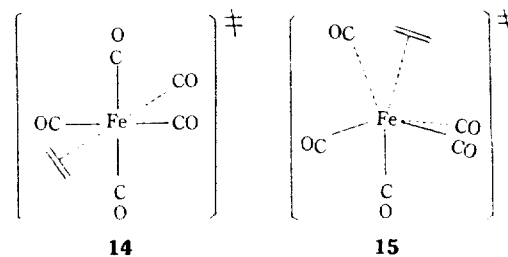
elude very unstable intermediates would be to allow the Fe-C distances to increase or one carbonyl to remove. In order to finish a whole substitution process via an intermediate, 14 or 15, it requires at least three steps. The first step is to distort from trigonal bipyramid structure to 12 or 13, followed by the approach of ethylene to perturbed geometry. The last one is to remove one carbonyl from 14 or 15. The total energy for three step via 14 or 15 is 130.50 and 393.59 kcal/mol, respectively. Accordingly, among two intermediates, 14 and 15, the reaction mechanism via 15 will be ruled out due

Table I. Extended Hückel Calculation Parameters

atom	orbital	H_{ii}(eV)	ξ_{ii}	$(C_1)^a$	i2	$(C_2)^a$
Fe	4s	-9.10	1.9			
	4p	-5.32	1.9			
	3d	-12.6	5.35	(0.5505)	2.00	(0.6260)
C	2s	-21.4	1.625			
	2p	-11.4	1.625			
O	2s	-32.3	2.275			
	2p	-14.8	2.275			

^{a}C_1 and C_2 are coefficients in a double-ξ expansion.

to large energy requirement.

Proposed mechanism. In the substitution of Fe(CO)₅ by ethylene, we proposed five intermediates as plausible mechanisms. From our calculation, we would say that if the reaction proceeds with a dissociative mechanism, the favourable one is the attack of ethylene to square-planar Fe(CO)₄ fragment. On the other hand, in the case that the reaction proceeds with an associative mechanism, the favourable one is the attack of ethylene to C_{4v} Fe(CO)₅ fragment. The next problem is to determine which of two reaction mechanisms is the most favourable one. The solution may be derived from the calculation of total energy required to complete a whole process.

Recently, Lineberger and coworker[12] studied the electron affinity determination for the series Fe(CO)n. They obtained the Fe(CO)₄-CO bond dissociation energy 2.4 ± 0.5 eV, based on the difference between the thermochemical value for the dissociation of Fe(CO)₅ to Fe + 5CO and the value for dissociating Fe(CO)₄ to Fe + 4CO. Smith[13] studied the gas-phase thermal decomposition of iron pentacarbonyl. They obtained the Fe(CO)₄-CO bond dissociation energy 41.5 kcal/mol. Accordingly, it requires 41-56 kcal/mol in removing one carbonyl from Fe(CO)₅. The resulting unstable Fe(CO)₄ fragment is spontaneously transformed into a stable geometry, i.e., D_{4h} Fe(CO)₄ (16), T_d Fe(CO)₄ (17), or C_{2v} Fe(CO)₄ fragment (18)[14] with energy gain. Our calculation shows that the total energy of 16 and 17 is -907.53 and -907.65 eV, respectively. When ethylene approaches to the intermediates, 16

16   **17**   **18**
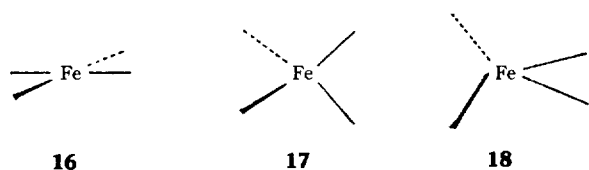
and 17, in bond length (2.25Å) it requires 23.53 and 42.8 kcal/mol, respectively. Therefore, among two possible reaction mechanisms, the reaction mechanism via 17 will be ruled out due to large energy requirement. In conclusion, among two plausible reaction mechanism via a dissociative process, 16, or an associative process, 14, the most favourable reaction mechanism consists of the attack of ethylene to D_{4h} Fe(CO)₄ fragment via a dissociative mechanism because it requires 79.45 kcal/mol to complete a whole process compared with the energy 130.50 kcal/mol in the case of 14 via an associative mechanism.

Appendix. The Fe-C and C-O distances are based on the Fe(CO)₅ obtained by gas-phase electron diffraction studies[15].

The extended Hückel calculations[16] used a modified Wolfsberg-Helmholz formula with the parameters listed in Table I. Orbital exponents and H_{ii}'s for Fe was obtained from previous work.[17]

References

1. F. A. Cotton and G. Wilkinson, Advanced Inorganic Chemistry, Interscience, Fouth Ed., p. 1183.
2. F. Basolo and R.G. Pearson, Mechanisms of Inorganic Reactions, Wiley, p. 124.
3. (a) G. R. Dobson, *Accts. Chem. Res.* **9**, 300 (1976); (b) J. A. S. Dobson, P. M. Burkinshaw, *Chem. Rev.,* **83**, 557 (1983).
4. (a) F. Basolo, *Inorg. Chim. Acta.,* **50**, 65 (1981); (b) F. Basolo, *Inorg. Chim. Acta.,* **100**, 33 (1985).
5. (a) M. I. Davis and C. S. Speed, *J. Organomet. Chem.,* **21**, 401 (1970); (b) B. Beagley, D. G. Schmidling and D. W. J. Cruickshank, *Acta. Crystallogr.,* **B29**, 1488 (1973); (c) H. D. Murdoch and E. Weiss, *Helv. Chim. Acta.,* **46**, 1588 (1963); (d) A. J. Carty, W. F. Smith and N. J. Taylor, *J. Organomet. Chem.,* **146**, C1 (1978); (e) F. A. Cotton and P. Lahuerta, *Inorg. Chem.,* **14**, 116 (1975); (f) C. L. Raston, D. Wege and A. H. White, *Aust. J. Chem.,* **30**, 2153 (1977); (g) R. Guilard and Y. Dusausoy, *J. Organomet. Chem.,* **77**, 393 (1974).
6. T. A. Albright, R. Hoffmann, J. C. Thibeault, and D. L. Thorn, *J. Am. Chem. Soc.,* **101**, 3801 (1979).
7. (a) J. R. Preer and H. B. Gray, *J. Amer. Chem. Soc.,* **92**, 7306 (1970); (b) M. Elian and R. Hoffmann, *Inorg. Chem.* **14**, 1058 (1975).
8. (a) T. A. Albright, J. K. Burdett and M. H. Whangbo, Orbital Interaction in Chemistry, Wiley-Interscience, 1985, p. 277; (b) M. Elian and R. Hoffmann, *Inorg. Chem.,* **14**, 1058 (1975).
9. (a) D. Bright and O. S. Mills, *J. Chem. Soc.* A, 1979 (1971); (b) J. Browing, M. Green, B. R. Penfold, J. L. Spencer, and F. G. A. Stone, *J. Chem. Soc., Chem. Sommun.,* 31 (1973).; (c) F. A. Cotton and P. Lahuerta, *Inorg. Chem.,* **14**, 116 (1975); (d) A. R. Luxmoore and M. Truter, *Acta. Crystallogr.,* **15**, 1117 (1962); (e) K. W. Muir and J. A. Ibers, *J. Organomet. Chem.,* **18**, 175 (1969); (f) T. H. Whitesides, R. W. Slaven, and J. C. Calabrese, *Inorg. Chem.,* **13**, 1895 (1974).
10. (a) C. Nave and M. R. Truter, *Chem. Commun.,* 1253 (1971); (b) M. O. Visscher, J. C. Huffman, and W. E. Streib, *Inorg. Chem.,* **13**, 792 (1974).
11. B. H. Weiller, M. E. Miller, and E. R. Grant, *J. Am. Chem. Soc.,* **109**, 352 (1987).
12. P. C. Engelking and W. C. Lineberger, *J. Am. Chem. Soc.,* **101**, 5569 (1979).
13. K. E. Lewis, D. M. Golden, and G. P. Smith, *J. Am. Chem. Soc.,* **106**, 3905 (1984).
14. (a) M. Poliakoff and J. J. Turner, *J. Chem. Soc., Dalton Trans.,* 1974, 2276; (b) J. K. Burdett, *Coord. Chem. Rev.,* **27**, 1 (1978); (c) G. A. Ozin and A. V. Voet, *Prog. Inorg. Chem.,* **19**, 105 (1975).

15. M. I. Davis and C. S. Speed, *J. Organomet. Chem.*, **21**, 401 (1970).

16. R. Hoffmann, W. N. Lipscomb, *J. Chem. Phys.*, **36**, 2179

(1962).

17. R. H. Summerville, R. Hoffmann, *J. Am. Chem. Soc.*, **98**, 7240 (1976).

An Improved Method of Pore Size Distribution Analysis

Hyun-Woo Cho and Woon-Sun Ahn*

Department of Chemistry, Sung Kyun Kwan University Suwon 440-746

G. D. Halsey

Department of Chemistry, University of Washington, Seattle, WA 98195, U.S.A. Received November 18, 1987

An improvement over the method of pore size distribution analysis has been made in this work. The improved method is based upon the idea of the micro pore analysis of Mikhail, Brunauer, and Bodor, and utilizes the V-t curve of nitrogen adsorption. Two pore models are assumed, and the deviation of the initial slope of the V-t plot is ascribed to the pore filling and to the adsorption on the wall of unfilled pores. The improved method of this work is very convenient in that the analysis starts from the small pore regions. The method of this work is however quite distinct from the similar V-t plot method proposed by Sellevold and Radjy. The proposed method is applied to a few adsorbents, and very satisfactory results are obtained. The cumulative surface area calculated by this method also agrees very well with those obtained by the BET plot or by the t-method.

Introduction

The t-method, put forward originally by Lippens and deBoer[1], has been applied quite extensively in evaluating the surface area of solid adsorbent. The method was further developed to apply to the micro pore analysis by Mikhail, Brunauer, and Bodor[2], and later to the meso pore distribution analysis by Sellevold and Radjy[3,4]. The meso pores are assumed to be either slate-shaped or open-ended circularly cylindrical in their work. In this meso pore analysis method, like in any other adsorption isotherm methods[5,6], the volume of nitrogen adsorbed in a small finite pressure range is assumed to consist of two contributions, one due to the pore condensation if any and the other due to the adsorption on empty pore walls. In case of slate-shaped pores, the surface area of the adsorbent decreases with increase in vapor pressure of the adsorbate gas as a consequence of the pore filling by the growing statistical thickness. In case of cylindrical pores on the other hand, the pore condensation takes place. It is necessary therefore to know the average radius of pores in which the condensation takes place as a function of the vapor pressure and the statistical thickness just prior to the condensation. Sellevold and Radjy made a few assumptions in order to calculate these. First of all, they introduced an idea of effective thickness. The thickness of the physorbed layer calculated from this effective thickness is expected to give an unreasonably small value, and moreover they ignored the curvature effect of adsorbent surface on the thickness of physisorption. They assumed furthermore a fictitious distinction between the condensate and the physisorbed layer. Nevertheless, this method is quite attractive in that the analysis starts from small pore regions rather than from the large pore regions.

In the improved method, the average radius of the pores in which the condensation takes place in a given small vapor pressure range and the average statistical thickness just prior to the condensation may be calculated using any one of the universal adsorption isotherms in which the Kelvin condensation term is introduced[7,8]. The Frenkel-Hill-Halsey equation[9] is used as an universal isotherm in this work.

Meanwhile the volume of the pore condensate can be estimated from the deviation of the slope of initial straight line of the V-t plot. These knowledges will be sufficient to know the volume and the wall area of the pores in which the condensation takes place.

The improved method proposed in this work is based upon the idea of the micro pore analysis by Mikhail, Brunauer, and Bodor, and will provide a means by which the pore volume distribution can be estimated as a function of the pore radius in the meso pore range. The improved method assumes none of above assumptions made by Sellevold and Radjy, and the results of analysis by this method are quite satisfactory when they are compared with the results obtained by conventional adsorption isotherm method.

Theory and Results

The Slope of the V-t plot. Experimental isotherms of nitrogen physisorption on high energy non-porous solid surfaces (such as metal oxide) at the liquid nitrogen temperature are found to be very similar in shape[10]. It stimulated many investigators to seek for an universal adsorption isotherm. The FHH equation in the following form can be regarded as one of them.

$$\ln(p^{o}/p) = b/\theta^{s} \tag{1}$$